International Journal of Multidisciplinary Research and Growth Evaluation.

Mapping Landslide Susceptibility Areas in Onitsha Metropolis of Anambra State Nigeria Using GIS

Nkanu BI [1*], Emengini EJ [2], Idhoko KE [3]
[1-3] Department of Surveying and Geoinformatics, Nnamdi Azikiwe University Awka, Nigeria

* Corresponding Author: **Nkanu BI**

Article Info

ISSN (Online): 2582-7138
Impact Factor (RSIF): 8.04
Volume: 07
Issue: 03
May-June 2026
Received: 07-03-2026
Accepted: 05-04-2026
Published: 03-05-2026
Page No: 452-471

Abstract
Landslides constitute one of the most destructive geomorphic processes, exerting far-reaching socio-economic and environmental impacts in susceptible regions worldwide. The frequency and magnitude of landslide occurrences have increased significantly in recent decades, driven by evolving climatic patterns and intensifying anthropogenic interventions on environmentally sensitive terrains. This study is aimed at a GIS based landslide susceptibility mapping of Onitsha north local government area, Anambra State Nigeria. The objectives of the study are to; identify and characterize the key physical factors contributing to landslide occurrences in Onitsha Metropolis; evaluate and rank these factors according to their level of influence; systematically classify the factors into distinct levels of susceptibility and delineate and map the landslide-susceptible areas within Onitsha Metropolis. The methodology incorporated seven conditioning factors: slope, elevation, rainfall, aspect, soil, curvature and geology. Spatial datasets were standardized, reclassified, and weighted using analytical hierarchy process (AHP) to produce a composite landslide susceptibility index. The results generated through Weighted Linear Combination (WLC) analysis delineated four risk zones: Very Low Risk, Low Risk, Moderate Risk and High Risk. The landslide susceptibility analysis showed that very low-risk zones constituted only 0.36% (0.147 km²) of Onitsha Metropolis, primarily located on flat valley bottoms and depositional surfaces where slope-driven processes are minimal. Low-risk zones covered 45.40% (18.747 km²), occurring on gently undulating terrain with limited slope-induced gravitational forces, offering relative safety for development when supported by proper drainage and slope management. Moderate-risk zones accounted for the largest proportion, covering 50.82% (20.985 km²). These areas, found on transitional slopes and concave landforms, are moderately stable but prone to landslides under persistent rainfall or anthropogenic alteration. High-risk zones spanned 3.42% (1.414 km²), concentrated along steep slopes and poorly drained hill flanks characterized by topographic instability. Spatial overlay with settlement areas revealed that GRA, Okpoko, Army Barracks, and Nkwelle were located within very high-risk zones, necessitating urgent mitigation measures. Conversely, Trans Nkisi, Umuaroli, Omogba, Fegge, and Odoakpu were situated in moderate-risk zones, where preventive land-use planning and slope monitoring are recommended.

Keywords: Landslide susceptibility mapping, Geographic Information System (GIS), Analytical Hierarchy Process (AHP), weighted overlay analysis, slope instability, remote sensing, geospatial analysis

1. Introduction
Landslides represent a major environmental and geomorphological hazard that continues to threaten human settlements, infrastructure, and ecological systems in many parts of the world, particularly within mountainous, hilly, and rapidly urbanizing terrains. The occurrence of landslides is associated with the interaction of several natural and anthropogenic factors, including lithology, slope gradient, soil characteristics, rainfall intensity, vegetation cover, drainage conditions, and human activities such

as excavation, deforestation, and uncontrolled urban development. Slope instability occurs when the gravitational forces acting on earth materials exceed their shear strength, resulting in the downslope movement of soil, rock, or debris. Extreme rainfall events, seismic activities, land degradation, and poorly regulated land use practices have been identified as major triggers of landslide events in many vulnerable environments (Metternicht, Hurni, and Gogu, 2005) [6]. The increasing frequency of climate-related extreme weather conditions and expanding human pressure on fragile landscapes have further intensified the occurrence of landslides globally, thereby increasing concerns regarding environmental sustainability and disaster risk management.

Advancements in geospatial technologies have significantly improved the capability to investigate, monitor, and predict landslide-prone environments. Geographic Information Systems (GIS), remote sensing techniques, and spatial modelling approaches now provide reliable platforms for integrating large volumes of environmental data for hazard assessment and decision-making. These technologies facilitate the extraction and analysis of terrain characteristics, hydrological parameters, geological structures, and land cover dynamics that influence slope instability. Through the integration of spatial datasets and analytical models, GIS-based landslide susceptibility mapping has become an effective approach for identifying vulnerable areas and supporting hazard mitigation planning (Ulakpa, Okwu, Chukwu, and Eyankware, 2020) [15]. Multi-criteria decision-making techniques combined with geospatial analysis have also enhanced the accuracy of landslide prediction by enabling the evaluation of multiple conditioning factors within a unified analytical framework.

Across southeastern Nigeria, several studies have demonstrated the applicability of GIS and remote sensing techniques in assessing landslide susceptibility and slope instability. Research conducted within the Iva Valley area employed heuristic and bivariate statistical approaches to generate landslide susceptibility maps that supported environmental management and land use planning initiatives (Ozioko and Igwe, 2020) [13]. Similar investigations in other parts of southeastern Nigeria applied statistical models and machine learning algorithms to examine the influence of terrain attributes, geology, rainfall variability, land cover changes, and soil properties on landslide occurrence (Amah *et al*., 2020; Nnanwuba, Nwosu, Okeke, and Ezeh, 2022) [1, 9]. Additional studies incorporating advanced machine learning algorithms such as Random Forest and Naïve Bayes achieved improved predictive accuracy through the integration of high-resolution spatial datasets and automated classification techniques (Ayadiuno, Ndulue, Mozie, and Ndichie, 2021; Nebeokike, Igwe, Egbueri, and Ifediegwu, 2020) [2, 7]. These investigations collectively demonstrate the growing relevance of geospatial modelling approaches in understanding slope instability patterns and hazard distribution within southeastern Nigeria.

Onitsha Metropolis in Anambra State has experienced rapid urban expansion, population increase, and extensive infrastructural development over recent decades. These changes have significantly transformed the natural landscape through vegetation removal, alteration of drainage pathways, soil disturbance, and increased impervious surface coverage. Although global hazard assessment platforms such as Think Hazard categorize the area as having very low landslide susceptibility, such generalized assessments are often based on coarse-resolution datasets that may not adequately capture localized terrain variability and anthropogenic influences (Hall, Huang, Timokhin, and Hammel, 2020) [3]. Urban growth within densely populated environments frequently modifies natural hydrological systems, intensifies surface runoff, and accelerates erosion processes, particularly within areas characterized by weak sedimentary formations and unstable soil conditions (Luo, Chen, Zhang, and Wang, 2022) [5]. Consequently, the interaction between rapid urbanization, modified drainage networks, residual slopes, and heterogeneous geological conditions may increase localized susceptibility to slope instability within Onitsha North.

Despite the increasing number of regional studies on landslide susceptibility assessment in southeastern Nigeria, detailed investigations focusing specifically on Onitsha North remain limited. Existing regional analyses provide valuable insights into the spatial distribution of landslide hazards; however, they often fail to adequately represent localized environmental and anthropogenic conditions associated with rapidly urbanizing urban centres. The complex interaction between land use change, drainage modification, geological variability, and urban infrastructure development within Onitsha North necessitates a location-specific assessment capable of identifying areas vulnerable to slope instability. A detailed GIS-based landslide susceptibility assessment is therefore required to provide reliable spatial information for environmental planning, hazard mitigation, urban development control, and sustainable land management within the study area.

2. Materials and Methods

2.1. Study area

Onitsha Metropolis is situated in the southeastern part of Nigeria, within Anambra State. It is located between latitudes 6°6'N and 6°12'N and longitudes 6° 46' 30" E and 6°49' 30" E. The area is characterized by a high population density and a vibrant urban environment, with a mix of residential, commercial, and industrial zones. Onitsha Metropolis lies within the humid tropical climatic belt of southeastern Nigeria and exhibits characteristics of the tropical wet and dry climate classified as Aw under the Köppen system. Seasonal rainfall distribution in the region is influenced by the oscillation of the Intertropical Convergence Zone, resulting in two dominant seasons comprising a wet season extending approximately from March or April to October and a dry season from November to February. Climatic investigations across Anambra State indicate that the region experiences warm humid conditions with annual rainfall typically ranging between about 1,520 mm and 2,020 mm, reflecting strong monsoonal influence (Ifeka and Akinbobola, 2015; Nnadi, 2019) [4, 8].

Rainfall analyses specifically conducted for Onitsha show mean annual precipitation values close to 1,850 mm, confirming the humid tropical nature of the area. Temperature conditions remain high throughout the year, with mean annual values generally between approximately 23°C and 37°C, while relative humidity remains elevated, particularly during the rainy season (Okeke, Eze, and Nwankwo, 2019) [11].

Long-term rainfall variability studies further reveal that Onitsha experiences significant seasonal rainfall peaks between June and September, accompanied by high moisture availability and intense convective storms. These climatic conditions enhance vegetation growth but also contribute to surface runoff generation, soil saturation, and geomorphic processes such as erosion and slope instability (Obeta, 2022; Oloruntade, 2018) [10, 12].

2.2. Methodology

The methodology adopted for this study integrated geospatial analysis and multi-criteria decision-making techniques for the assessment and mapping of landslide susceptibility within the study area. The analytical framework commenced with comprehensive data preprocessing procedures aimed at improving the accuracy, consistency, and reliability of the acquired spatial datasets. Satellite imagery and ancillary datasets were subjected to radiometric calibration to correct sensor-related variations, while geometric rectification was carried out to eliminate distortions resulting from Earth rotation, terrain displacement, and sensor geometry. Subsequently, all datasets were reprojected into the Universal Transverse Mercator (UTM) Zone 32N coordinate system using Ground Control Points (GCPs) to ensure spatial compatibility and precise geo-referencing across all thematic layers.

SRTM processing was then undertaken to establish an accurate representation of the terrain characteristics of the study area. The DEM dataset was examined for topographic inconsistencies such as depressions and artificial sinks that could affect hydrological and terrain analysis. Sink-filling algorithms implemented within ArcGIS Pro were used to remove these anomalies and generate a hydrologically corrected DEM surface. Following correction, terrain derivatives including slope, aspect, and curvature maps were generated to describe the terrain morphology and topographic variability influencing landslide occurrence. These terrain parameters provided important information regarding slope steepness, directional orientation, and surface curvature, which are widely recognized as significant controls on slope instability and mass movement processes.

Thereafter, thematic factors associated with landslide susceptibility, including slope, elevation, aspect, curvature, rainfall, soil type, geology, and land cover, were classified and standardized into susceptibility categories according to their relative influence on landslide occurrence. Each factor layer was reclassified into different risk levels ranging from low to high susceptibility using established classification criteria obtained from literature and expert knowledge. This standardization process ensured that all variables were represented on a common analytical scale, thereby facilitating integration and comparison within the multi-criteria evaluation framework.

The Analytical Hierarchy Process (AHP) was subsequently employed to determine the relative importance of the selected landslide conditioning factors. Pairwise comparison matrices were developed through expert judgment and literature-based evaluation using Saaty's numerical scale ranging from 1 to 9. Each factor was systematically compared against others to establish its level of influence on landslide occurrence. The pairwise comparison matrices were then normalized, and criterion weights were computed through eigenvector analysis. The derived weights represented the relative contribution of each factor to landslide susceptibility within the study area. To ensure the reliability and logical consistency of the judgments used in the weighting process, the Consistency Ratio (CR) and Consistency Index (CI) were calculated. A consistency ratio below the acceptable threshold of 0.1 confirmed the adequacy and reliability of the assigned weights.

Following the derivation of factor weights, weighted overlay analysis was conducted within a Geographic Information System (GIS) environment to integrate all thematic layers into a composite landslide susceptibility model. Each standardized factor layer was multiplied by its corresponding AHP-derived weight, and the weighted layers were combined using raster overlay operations to generate a landslide susceptibility index map. The resulting index was subsequently classified into different susceptibility zones, including very low, low, moderate, high, and very high landslide risk categories. The final susceptibility map provided a spatial representation of areas vulnerable to landslide occurrence and served as a decision-support tool for hazard mitigation, land use planning, environmental management, and disaster risk reduction within the study area.

3. Results

3.1. Identification and Characterization of Landslide Conditioning Factors

Landslide occurrence in Onitsha North is influenced by a complex interaction of geomorphological, geological, pedological, and climatic parameters. The following conditioning factors derived from spatial analysis were identified and characterized using Digital Elevation Model (DEM), slope, curvature, aspect, geology, soil, and rainfall datasets.

The DEM values within the study area ranged between 17 m and 163 m above mean sea level. The lower elevations are concentrated in the southern and southwestern sectors, corresponding to floodplains and depositional surfaces. The higher elevations are distributed towards the north and northeastern parts, associated with hilly terrains. Elevation is a fundamental control of slope stability, as higher grounds are generally linked with steeper gradients, runoff acceleration, and enhanced susceptibility to landslides, see Figure 1.

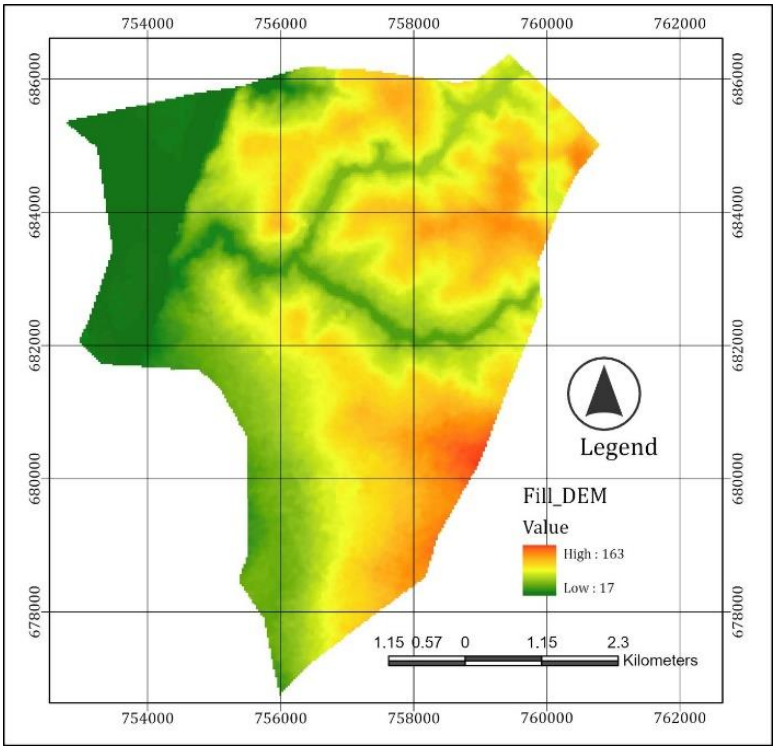

Fig 1: Elevation Data

The slope gradient (Figure 2) varies from 0° to 27.7°, with low slopes dominating central depressions and flat plains, while high slopes align with escarpments and river channel boundaries. Gentle slopes (0°–5°) are stable and less prone to failure, but moderate to steep slopes (15°–27°) are more vulnerable due to gravitational stress, runoff concentration, and soil erosion processes. Steep slope corridors, particularly those running parallel to drainage networks, represent high-risk zones for slope instability.

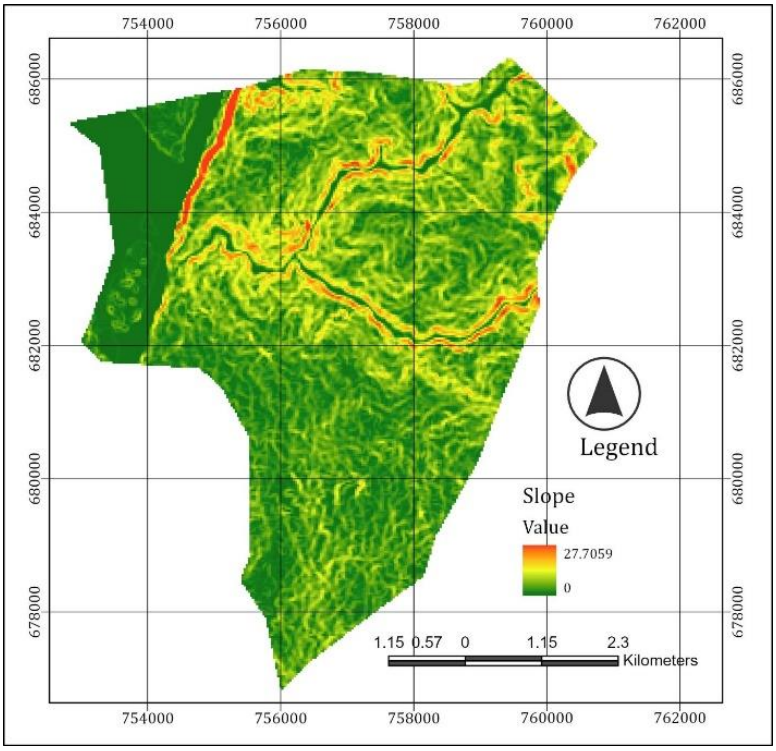

Fig 2: Slope Data

Curvature values in the area (Figure 3) range between -4.72 and +4.62, delineating concave and convex surfaces. Concave profiles (negative values) are associated with water accumulation zones, which favor infiltration and pore pressure build-up, leading to slope failure. Convex profiles (positive values) denote diverging slopes prone to surface runoff acceleration and soil wash. The dominance of near-flat curvature values indicates relatively stable surfaces, although local variations highlight potential landslide initiation points along concave depressions.

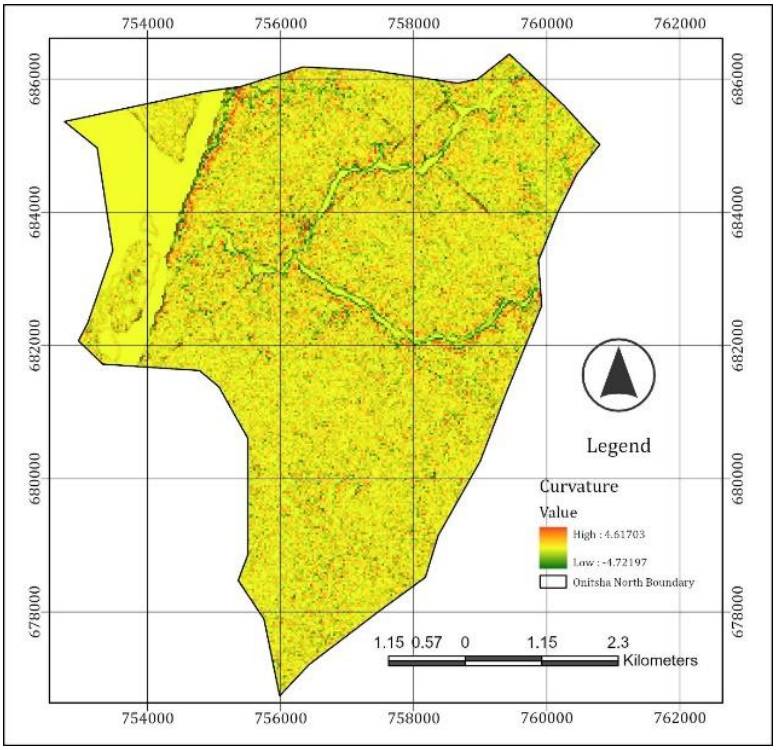

Fig 3: Curvature Data

The aspect map (Figure 4) reveals diverse slope orientations, categorized into flat, north, northeast, east, southeast, south, southwest, west, northwest, and north-facing slopes. Aspect determines insolation, evapotranspiration, and moisture retention, which in turn influence vegetation cover and soil stability. South-facing slopes tend to experience higher evaporation rates, making soils drier and more prone to landslides, while north-facing slopes retain more moisture, promoting saturation and slope instability under heavy rainfall. The heterogeneity of aspect distribution indicates spatial variability in landslide susceptibility across the area.

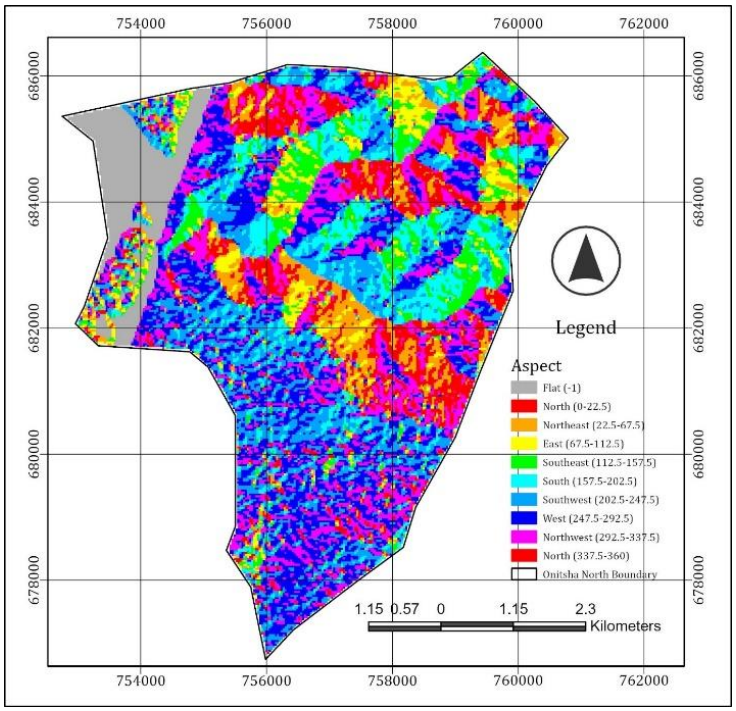

Fig 4: Aspect Data

The geological framework (Figure 5) is dominated by siliciclastic sedimentary rocks forming high hills and Tablelands with considerable relief. Flat or nearly flat plains occupy localized depressions, while smaller portions are characterized by surface water bodies. The lithology of siliciclastic sediments is generally friable and prone to weathering, which weakens slope materials and increases landslide susceptibility. The juxtaposition of high-relief Tablelands with adjacent low-lying plains further enhances slope instability risks.

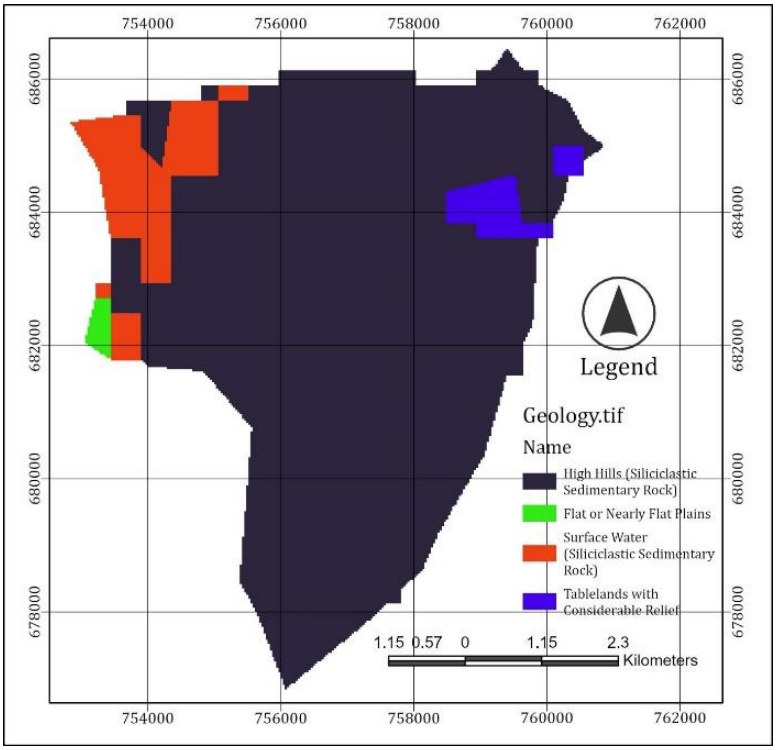

Fig 5: Geologic Data

Soil types identified include sandy clay, clay loam, sandy clay loam, and silt. Sandy clay loam covers most of the area (Figure 6), characterized by moderate cohesion and drainage, but its erodibility increases under high rainfall. Silt soils, though limited in extent, are highly unstable due to low cohesion and high susceptibility to erosion. Clay loam soils provide moderate stability due to higher cohesion, although water saturation under prolonged rainfall may weaken them significantly. Soil texture and structure directly influence shear strength, infiltration capacity, and overall landslide potential.

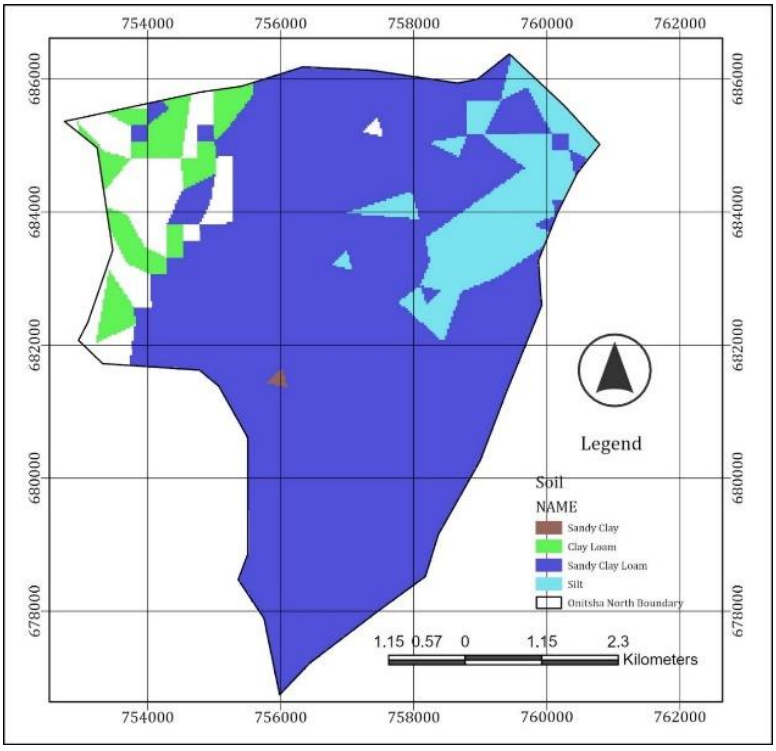

Fig 6: Soil Data

Rainfall distribution across the study area ranges from 2,844.26 mm to 2,906.37 mm annually (Figure 4.7). The southeastern and southern regions record the highest values, correlating with zones of steep slopes and erodible soils. High rainfall accelerates the processes of infiltration, runoff, and pore water pressure build-up, all of which contribute to slope failures. Seasonal variability, with peak intensities during the wet months, further enhances the risk of rainfall-induced landslides.

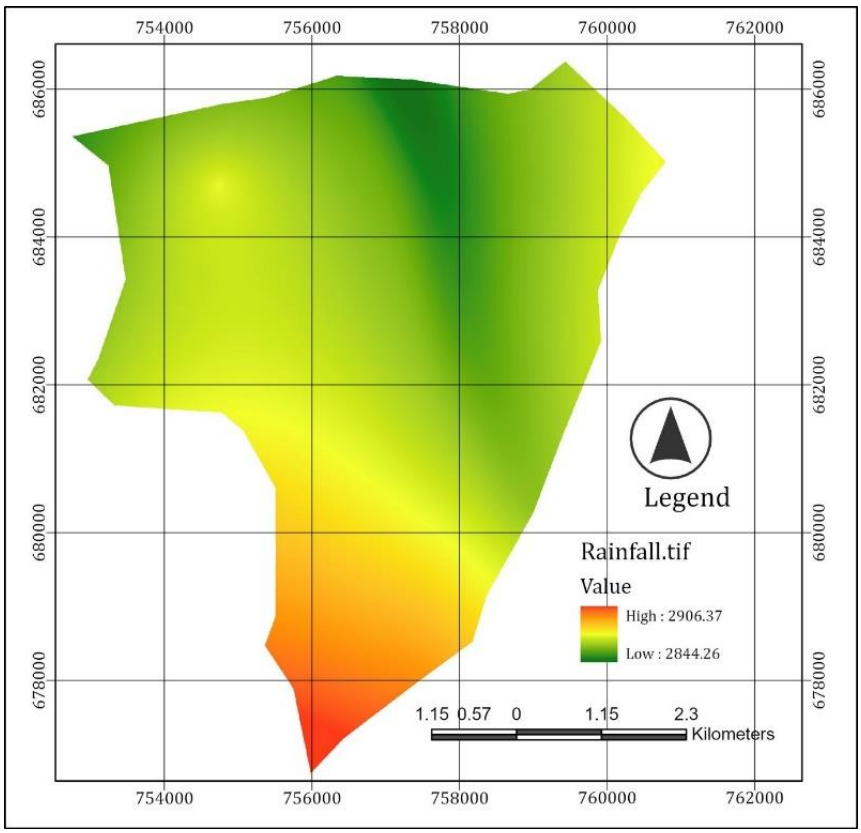

Fig 7: Rainfall Data

Spatial overlays (Figure 1 – 7) show that the steepest slopes occur along the flanks of the elevated Tablelands and along entrenched drainage corridors. These same corridors are marked by negative curvature values, indicating convergent flow and a tendency for groundwater mounding during storms. Sandy clay loam covers most of these belts, which increases the likelihood of surface wash and shallow slip detachment once cohesion is reduced by saturation. The southern sector registers the highest annual rainfall, aligning with several steep, convergent tracts, so storm-driven pore-pressure rise is expected to be strongest there. Low-lying plains in the west and southwest display gentle slopes, near-zero curvature, and a higher proportion of clay loam. Those sectors are comparatively stable with respect to slope failure, although bank undercutting and gully expansion can still occur along channel margins during peak discharges.

Overall patterns are consistent with process-based expectations from the landslide literature. Elevation establishes the relief framework, slope furnishes the gravitational driver, curvature structures water convergence and divergence, aspect modulates antecedent moisture and vegetation, geology sets shear behaviour and structural anisotropy, soil governs drainage and cohesion, and rainfall provides the hydrologic forcing. Areas where steep gradients intersect concave topography within siliciclastic regoliths of sandy clay loam under high rainfall emerge as the most failure-prone tracts within Onitsha North. A summary of the thematic layers, their data sources, derivation techniques, and justification for inclusion is presented in Table 1.

Table 1: Summary of Landslide Conditioning Factors and Justification for Inclusion

S/N	Thematic Layer	Source/Derivation Method	Relevance to Landslide Assessment
1	DEM (Elevation: 17–163 m)	www.earthexplorer.usgs.gov Hydrologically corrected DEM produced with a sink-fill operation and clipped to the Onitsha North boundary	Establishes relief and potential energy, supplies the parent surface for all terrain derivatives, and frames zones where gravitational driving stresses increase with local relief
2	Slope (0–27.7°)	Computed from the filled DEM using a standard 3×3 finite-difference algorithm in degrees	Represents the primary mechanical driver of instability because shear stress rises with gradient and runout potential increases along steep belts adjacent to drainage corridors
3	Curvature (−4.72197 to 4.61703)	Calculated from second derivatives of the DEM as general curvature and mapped as a continuous raster	Differentiates convergent hollows with negative curvature that favour saturation and pore-pressure rise from convex noses where divergent flow accelerates surface wash and soil thinning
4	Aspect (Flat; N, NE, E, SE, S, SW, W, NW; NNW)	Derived from the DEM aspect grid and reclassified into nine directional classes and a flat class	Modulates insolation, evapotranspiration, antecedent moisture, and vegetation cover, thereby altering shear strength and hydrologic response during storms across opposing hillsides
5	Geology (siliciclastic sedimentary terrains: high hills, Tablelands with relief, nearly flat plains; surface water)	Geological map generalized and rasterized to analysis grid and clipped to the municipal boundary	Constrains material properties, bedding and weakness orientations, and slope-break architecture that localize translational sliding and debris slips on sedimentary sequences
6	Soil (sandy clay loam, clay loam, sandy clay, silt)	www.isric.org Soil polygon data harmonized and converted to a categorical raster	Governs drainage, permeability, and cohesion; sandy clay loam and silt exhibit higher erodibility and lower shear strength under saturation compared with clay-richer units
7	Rainfall (2,844.26–2,906.37 mm)	www.chc.ucsb.edu Chirps Gridded climatological rainfall surface prepared for the study area and clipped to the boundary	Provides hydrologic forcing that elevates pore pressure and triggers shallow failures, with higher totals coinciding with steep, convergent hillslope tracts

Source author, 2025

3.2. Reclassification and Standardization of Landslide Conditioning Factors

A five-class ordinal scale was adopted for all conditioning factors, where 1 denotes Very Low Risk and 5 denotes Very High Risk. Thresholds were selected to reflect established process relationships among topography, hydrology, materials, and triggering rainfall, while maintaining transparent, reproducible breakpoints for raster implementation. Slope, curvature, and aspect encode mechanical and hydrological controls on detachment and pore pressure; elevation frames relief and potential energy; geology and soil set shear behaviour and erodibility; rainfall provides hydrologic forcing. In this study, seven critical conditioning factors were reclassified into a common susceptibility scale ranging from 1 to 5, with the following interpretations:

1. corresponds to Very Low Risk,
2. corresponds to Low Risk,
3. corresponds to Moderate Risk,
4. corresponds to High Risk, and
5. corresponds to Very High Risk.

The reclassification process was implemented in a GIS environment using reclassify tools. Elevation structures relief and controls potential energy available for downslope movement. Higher positions in this landscape coincide with steeper flanks and stronger hydraulic gradients, which raise driving stresses and favor rapid saturation along convergent elements. Topography conditions shallow landslide initiation through the joint action of slope and subsurface flow pathways.

The elevation Table (Table 2) partitions the study area's relief from 17 m to 163 m into five equal-interval classes that increase monotonically in landslide predisposition from Very Low to Very High risk. Equal-interval discretization was adopted because the local hypsometric range is modest and approximately continuous, so fixed 29.2 m steps provide transparent thresholds while preserving the expected positive relation between altitude and relief in this terrain. Elevation is not a trigger by itself; it operates as a proxy for relief and for the likelihood of steep valley flanks and dissected interfluves, where gravitational driving stresses and hydraulic gradients tend to be greater. Numerous inventories and reviews report elevation among the recurrent predictors of landslide occurrence, typically because higher ground in dissected landscapes co-occurs with steeper slopes and concentrated drainage networks.

Class 1 (17.0–46.2 m) represents the low-lying plains and valley bottoms where local relief is small. Gravitational forcing is limited, so slope-related failures are comparatively uncommon, although fluvial undercutting and sediment mobilization can occur along channels. Empirical studies generally report lower landslide densities in such low-relief belts.

Class 2 (>46.2–75.4 m) marks gentle rises and low interfluves where relief begins to increase. Susceptibility is higher than in the floodplain because short, locally steep facets appear near channel margins and road cuts, although extensive tracts still exhibit gentle gradients. Statistical models often show a gradual increase in landslide probability across these transitional belts.

Class 3 (>75.4–104.6 m) corresponds to intermediate elevations where slope breaks and short hillslopes become frequent. These mid-slope positions are where shallow colluvial failures typically initiate during intense storms because convergent subsurface flow raises pore water pressures while gravitational shear is already appreciable. Physically based models that couple topography with

subsurface flow predict higher failure likelihoods for such mid-elevation hollows and planar facets.

Class 4 (>104.6–133.8 m) captures high-relief sectors on interfluves and escarpment shoulders. The combination of longer, steeper hillslopes and greater drainage dissection increases driving stresses and reduces the stability margin under storm wetting. Guidelines and inventories consistently associate these settings with frequent shallow slides and debris slips in humid regions.

Class 5 (>133.8–163.0 m) isolates the highest ground and the steep valley sidewalls that descend from it. These facets present the strongest gravitational forcing and the most efficient runoff routing, which together favour rapid pore-pressure rise and shear failure during high-intensity rainfall. Both process models and empirical studies identify such high-relief belts as the most failure-prone portions of a landscape, see Table 2 and Figure 8.

Table 2: Elevation Reclassification Range

Risk class	Elevation range (m)	Rationale
1	17.0–46.2	Low relief plains with weak gravitational forcing
2	>46.2–75.4	Gentle rises where relief begins to increase
3	>75.4–104.6	Intermediate relief with more abundant slope breaks
4	>104.6–133.8	High relief sectors that commonly host steep facets
5	>133.8–163.0	Very high relief sectors that couple to steep valley flanks

Source author, 2025

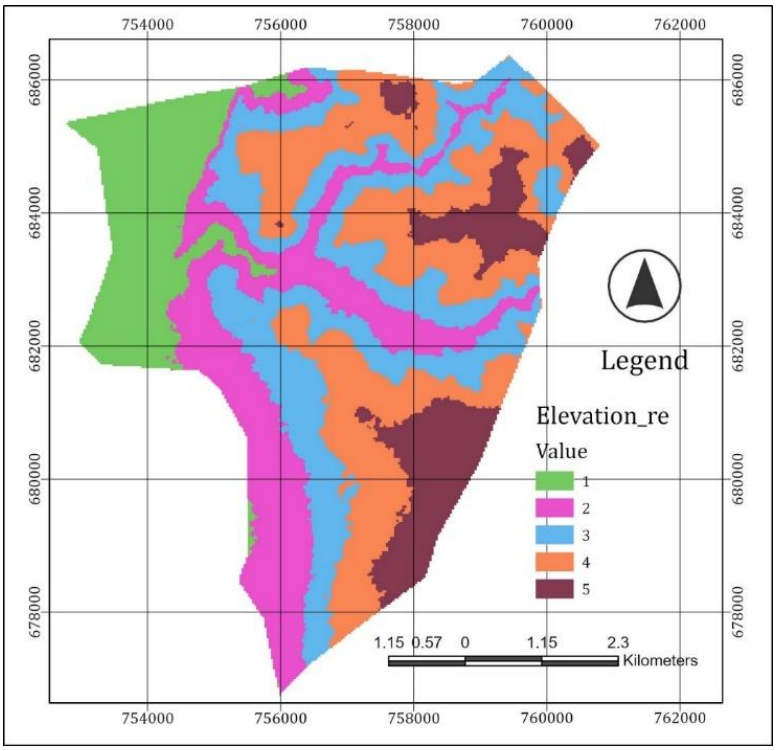

Fig 8: Reclassified Elevation Data

The slope angle is a primary mechanical driver of instability because shear stress rises with gradient. Frequencies of shallow landslides commonly increase from gentle to moderately steep terrain; five-degree classes provide informative discrimination for susceptibility mapping. The study area does not exceed about 28°, so a monotonic increase in risk with angle is appropriate. A graduated relationship between slope angle and landslide predisposition underpins the five-class scheme. Slope controls the magnitude of gravitational driving stress on soils and regolith, and its increase with angle is non-linear, so stability margins decline as gradients steepen, particularly during rainfall events that elevate pore water pressure. Widespread landslide inventories and reviews identify slope as one of the most informative predictors in susceptibility mapping, which supports the use of ordered classes for operational zoning.

Class 1, 0–5°, represents planar to very gentle terrain. Shear stresses are small, hydrologic residence times are long, and near-surface materials typically remain below failure thresholds except where bank undercutting or anthropogenic excavations locally increase stress. Empirical studies commonly report the lowest landslide densities in such topographically subdued belts.

Class 2, >5–10°, marks a transitional regime where runoff begins to concentrate and flow velocities increase. Localized oversteepening along road cuts, channel margins, or small convex breaks can permit shallow slips under intense rainfall, yet broad stability generally persists because effective stress losses remain limited outside convergent hollows. Guidance documents for land-use planning treat such gradients as low to moderate susceptibility zones when other factors are not adverse.

Class 3, >10–15°, corresponds to moderate slopes where failure likelihood rises markedly. Hydrologic forcing during storms increases pore pressure faster than it can dissipate, and the available gravitational stress begins to approach shear strength for common soil textures. Statistical and process-based studies show frequent shallow landslides initiating on

facets of this order, especially where plan or profile curvature focuses subsurface flow.

Class 4, >15–20°, aligns with steep terrain in which factors of safety often approach unity during prolonged or high-intensity rainfall. Longer slope lengths promote runoff acceleration and riling, root reinforcement can be insufficient to compensate for reduced effective stress, and small perturbations such as toe erosion or minor excavation may trigger failure. International guidelines and many regional inventories associate these gradients with high susceptibility in humid settings.

Class 5, >20–27.7°, captures the very steep end of the local distribution and therefore the strongest gravitational forcing in the municipality. These facets show the greatest coupling of rapid runoff, shallow saturation, and shear stress, producing frequent shallow slides and debris-slip activity during storm sequences. Recent analyses that include slope angle among multivariate predictors continue to find strong positive effects on landslide occurrence and, in some cases, on expected volume. See Table 3 and Figure 9.

Table 3: Slope Reclassification Range

Risk class	Slope range (degrees)	Rationale
1	0–5	Planar to very gentle slopes where driving stress is low
2	>5–10	Gentle slopes with limited shear but growing runoff energy
3	>10–15	Moderate slopes where shallow slips become more likely
4	>15–20	Steep slopes with reduced stability during storms
5	>20–27.7	Very steep slopes that concentrate runoff and fail readily

Source author, 2025

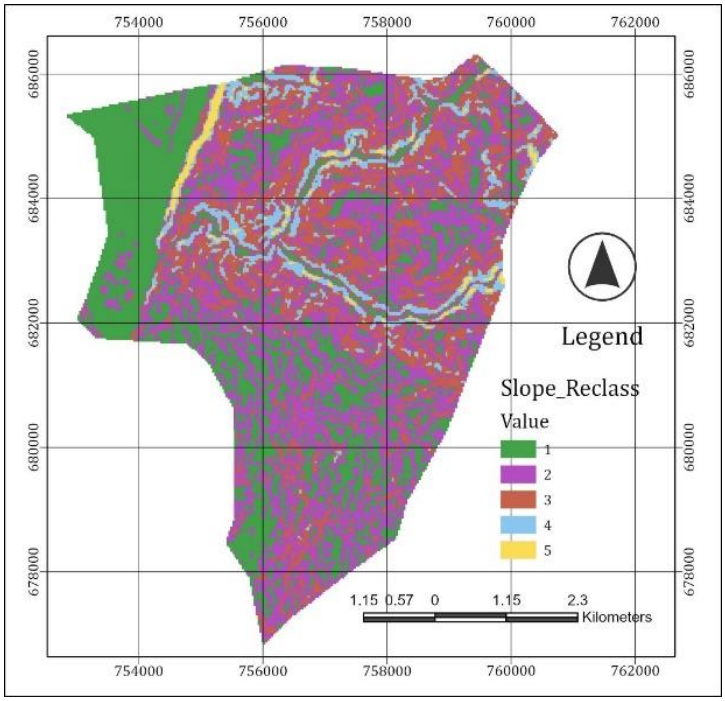

Fig 9: Reclassified Slope Data

Curvature partitions the study area into convergent hollows and divergent noses. Concave surfaces focus subsurface and surface fluxes, raise pore pressure, and promote failure, while convex surfaces disperse flow and favour soil thinning rather than saturation. Near-planar elements occupy an intermediate condition. Curvature quantifies the second derivative of the land surface and describes whether flow lines converge into hollows or diverge across noses. Positive values denote convex forms that disperse runoff and accelerate near-surface flow, whereas negative values denote concave forms that accumulate water and favour infiltration and transient groundwater mounding. Values near zero indicate planar elements with limited convergence or divergence.

The Table 4 adopts symmetric breakpoints around zero to partition hydrologic behaviour into divergent, planar, and convergent regimes. The near-planar band from −0.5 to +0.5 groups pixels where curvature magnitude is small relative to elevation noise at the working grid scale, which limits meaningful differentiation of hydrologic forcing. Moderately convex elements (>+0.5 to +2.0) and strongly convex noses (>+2.0) express increasingly efficient drainage and shorter water residence times, conditions that lower the likelihood of pore-pressure rise even on steeper slopes; such forms are therefore assigned Low and Very Low risk, respectively.

Moderately concave hollows (−2.0 to <−0.5) and strongly concave hollows (−4.72197 to <−2.0) represent progressively stronger topographic convergence. Convergent planforms concentrate subsurface and surface fluxes, increase capillary fringe thickness, and raise transient pore pressure during storms, which reduces effective stress and promotes shallow landslide initiation. Physically based and probabilistic models of shallow land sliding consistently predict elevated failure likelihoods in such hollows, and inventories report higher slide densities where curvature is markedly negative. The High and Very High classes in the Table therefore align with the hydrologic control exerted by topographic convergence on storm response, see Table 4 and Figure 10.

Table 4: Curvature Reclassification Range

Risk class	Curvature range	Rationale
1	>+2.0 to +4.61703	Strongly convex noses with divergent flow and limited saturation
2	>+0.5 to +2.0	Moderately convex elements with efficient drainage
3	−0.5 to +0.5	Near-planar surfaces with neutral hydrologic convergence
4	−2.0 to <−0.5	Moderately concave hollows that accumulate water
5	−4.72197 to <−2.0	Strongly concave hollows with focused saturation and high pore pressure

Source author, 2025

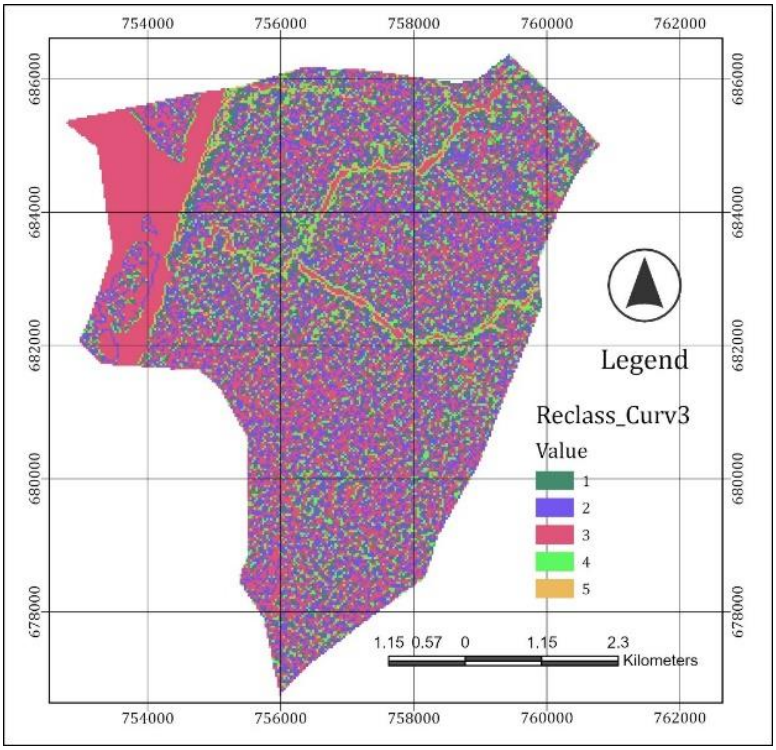

Fig 10: Reclassified Curvature Data

Aspect modulates insolation, evapotranspiration, and wind-driven rainfall exposure. Southern Nigeria experiences a humid monsoon with prevailing southwesterlies during the rainy season; windward slopes facing S–SW–W generally receive greater direct rainfall, while leeward facets dry faster but may retain moisture under shade depending on season. The classification therefore assigns higher risk to S–SW–W exposures and intermediate risk to N and E facets; flat pixels are least susceptible.

Aspect explains how slope orientation alters both microclimate and storm exposure, which together shape near-surface hydrologic response and shear strength. In humid monsoon climates of southern Nigeria, low-level southwesterlies dominate during the rainy season and transport moist Atlantic air inland, so slopes facing south and southwest receive more direct, windward rainfall and splash energy than lee or cross-wind facets. This climatological setting underpins the adopted ordering of risk in the aspect Table.

South and southwest aspects were assigned Very High risk because they align most directly with the prevailing south-westerly monsoon flow. Windward exposure promotes higher rainfall impingement and longer wetness duration, which increase transient pore pressures and reduce effective stress in shallow soils during storm sequences. Fundamental reviews of orographic precipitation and slope exposure explain why windward facets commonly register greater rainfall totals and cloud water inputs than leeward facets, even in low-relief terrain where local ridges still channel moist flow.

West and southeast aspects were mapped as High risk because they experience partial windward exposure and frequent cross-wind storm tracks in the study area. Afternoon convection and along-valley flows often approach from the west to southwest during the wet months, which raises the likelihood of rapid wetting, short recession times, and enhanced antecedent moisture relative to leeward orientations. Regional studies of the West African monsoon document westerly to south-westerly low-level inflow during boreal summer, supporting the elevated susceptibility assigned to these exposures.

North, east, and northwest aspects received Moderate risk because they occupy intermediate hydrometeorological conditions. North-facing slopes in the Northern Hemisphere tend to be cooler and wetter due to reduced insolation, which favours moisture retention after storms. East- and northwest-facing slopes receive mixed exposure to storm approach and variable diurnal radiation, producing neither strongly windward nor strongly leeward behavior. Empirical and experimental work shows that aspect systematically influences soil temperature and water content, with south-facing slopes typically warmer and drier and north-facing slopes cooler and moister, which justifies an intermediate susceptibility class for these orientations under the local monsoon regime.

Northeast aspects were placed in the Low risk class because they are most consistently leeward to the dominant south-westerly inflow during the wet season, which encourages

faster post-storm drying and shorter wetness durations. This assignment reflects the tendency for reduced windward impingement and lower splash erosion where storm approach is oblique or shielded by local relief. Contemporary susceptibility studies often encode aspect as directional predictors precisely to capture such microclimatic gradients, although the magnitude of aspect effects remains context dependent.

Flat terrain was assigned Very Low risk in the aspect layer because orientation has little meaning where slope is near zero. Such pixels usually coincide with planar valley bottoms or terraces in this dataset, where failure mechanisms relate more to fluvial undercutting or saturation from drainage impediments than to aspect-controlled wetting differences. Reviews of statistically based landslide susceptibility mapping include aspect among common predictors but note that its effect is contingent on relief, vegetation, and storm climatology, which is consistent with assigning minimal aspect-driven risk to flat classes, see Table 5 and Figure 11.

Table 5: Aspect Reclassification Range

Aspect class	Azimuth (degrees)	Risk class	Rationale
Flat	−1	1	No preferred exposure; usually gentle terrain
Northeast	22.5–67.5	2	Leeward to monsoon flow; higher insolation and faster drying
North	0–22.5 and 337.5–360	3	Potential moisture retention under reduced solar load
East	67.5–112.5	3	Intermediate wind exposure and drying
Northwest	292.5–337.5	3	Transitional exposure to storm tracks
West	247.5–292.5	4	Windward exposure to southwesterlies and splash erosion
Southeast	112.5–157.5	4	Transitional windward exposure with frequent storm impact
South	157.5–202.5	5	Direct exposure to moist monsoon storms
Southwest	202.5–247.5	5	Maximum windward exposure and rainfall impingement

Source author, 2025

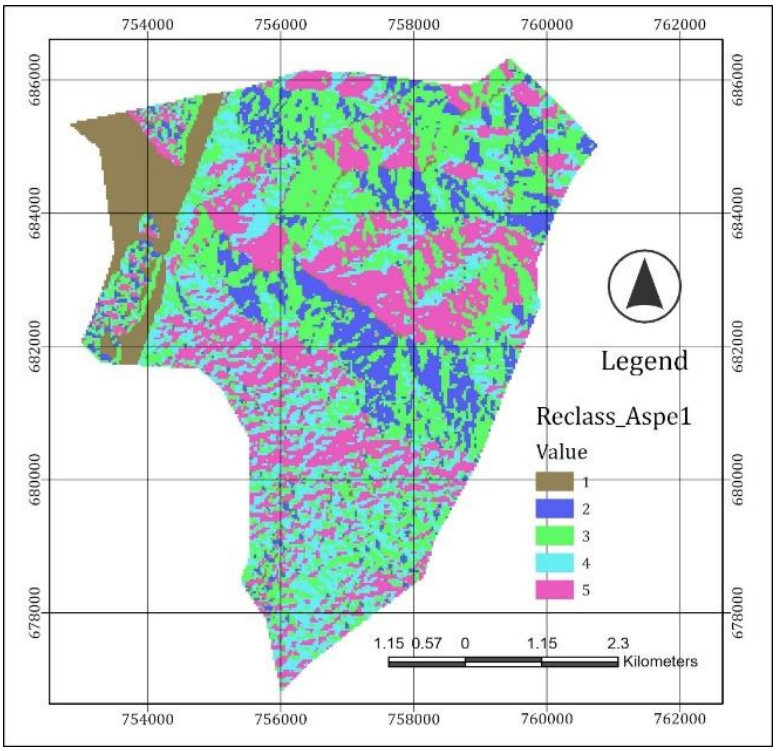

Fig 11: Reclassified Aspect Data

Geological classes were reinterpreted as proxies for material strength, structural anisotropy, and relief architecture, which together modulate shear resistance and the pathways for drainage and saturation. Siliciclastic sedimentary rocks dominate the municipality and weather to sandy and silty regoliths with variable cementation and interbeds of finer units. Such stratigraphy fosters perched water Tables and abrupt contrasts in permeability, conditions that lower effective stress during storm infiltration and predispose slopes to translational sliding along bedding or weak horizons. Regional case studies from the Nanka–Agulu sector of Anambra State document recurrent landslides and rapid gully enlargement where poorly consolidated sands overlie silty clay seams, with failures concentrated in the rainy season when pore pressures rise quickly.

High hills on siliciclastic sedimentary rocks were assigned Very High risk because that unit combines steep relief, thick weathered sand bodies, and bedding-parallel weakness planes. Field and laboratory investigations in the Anambra Basin show that Ajali and Nanka sands display low cohesion and high permeability relative to underlying clayey layers, promoting seepage faces and loss of matric suction during intense rainfall. Observations from multiple Nanka landslide sites indicate that heads carps develop on steep valley flanks and propagate downslope as translational slips or debris slides once saturation interfaces form at sand–silt contacts. The mapped high-hill belts provide the necessary gravitational forcing and exposure to storm-driven wetting to

maintain frequent failure activity.

Tablelands with considerable relief were classified as High risk because Table surfaces are generally well drained, whereas their margins host structural benches and scarps where bedding anisotropy aligns with slope aspect. Translational sliding preferentially localizes along caprock edges and stepped escarpments where lateral continuity of bedding promotes shear along weak horizons. International guidelines and mechanistic studies emphasise the role of bedding planes and relief contrasts in sedimentary terrains, noting elevated susceptibility where dip or sub horizontal stratification intersects steep slopes at the edges of plateaus and cuestas. The Anambra Basin literature reports similar behaviour where Tableland rims composed of ferruginous but variably cemented sands break into steep shoulders above clayey substrata.

Flat or nearly flat plains received Low risk because gravitational driving stresses are small and slope-parallel drainage is limited. Instability in these areas is more likely to arise from fluvial bank undercutting, piping, or anthropogenic excavation rather than from classic rainfall-triggered planar or rotational failures on hillslopes. Regional syntheses of gully erosion in Anambra State confirm that plains can experience bank collapses, although the dominant deep-seated or translational landslides concentrate on steeper siliciclastic hillsides. The classification therefore reduces the geology-driven susceptibility of plains while recognising that bank processes are treated separately through proximity-to-channels metrics.

Surface water polygons were assigned Very Low risk inside the landslide-geology layer because submerged pixels do not host slope failure in the same manner as subaerial hillsides. Bank retreat and scarping are important hazards at the land–water interface but are better represented through distance-to-channel or specific fluvial-erosion predictors rather than a lithological class. Professional guidance for susceptibility and hazard zoning supports exclusion or down weighting of permanent water bodies from the lithology-based failure domain, see Table 6 and Figure 12.

Table 6: Geologic Reclassification Range

Lithological–geomorphic unit	Risk class	Rationale
High hills on siliciclastic sedimentary rocks	5	High relief and weathered sandy–silty regoliths with weak planes
Tablelands with considerable relief	4	Stepped scarps and structural benches that localize sliding
Flat or nearly flat plains	2	Low relief and limited gravitational forcing
Surface water	1	Non-slope medium; bank erosion handled by separate proximity analysis

Source author, 2025

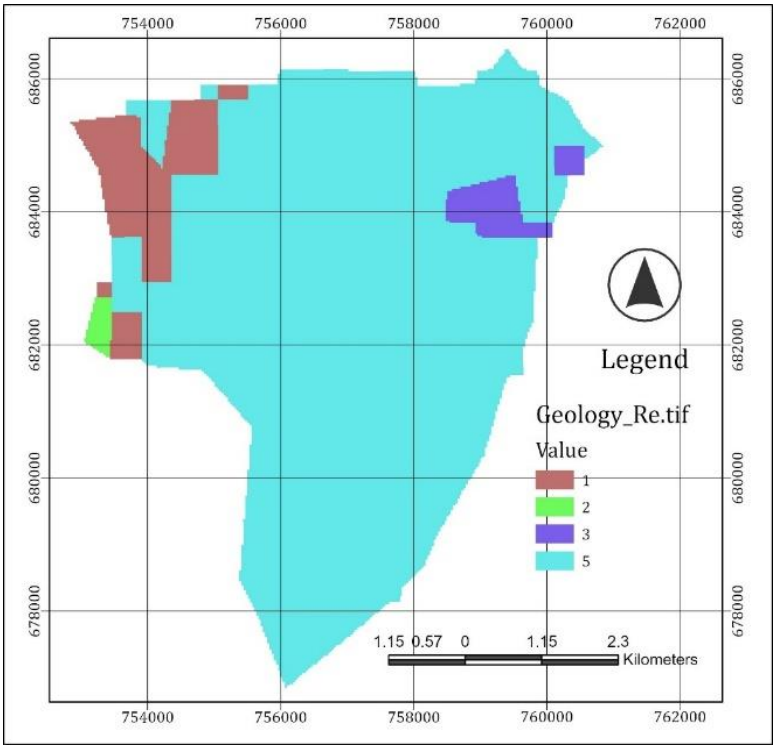

Fig 12: Reclassified Geologic Data

The soil was reclassified by their expected shear strength, permeability, and erodibility under intense rainfall, which together govern shallow-slope failure in humid monsoon settings. Unsaturated soil mechanics shows that matric suction contributes to shear strength in near-surface horizons, while storm infiltration reduces suction and lowers effective stress. Textures that transmit water rapidly or that exhibit low cohesion lose strength quickly during storms and therefore attract higher risk classes.

Silt receives Very High risk because silt-sized particles are readily detached and transported, and silty materials possess comparatively low cohesion. Experimental and empirical work on erodibility identifies silt as the most easily eroded fraction, with soils becoming less erodible as either the sand or clay fraction increases. Silty horizons also display moderate to relatively low permeability that promotes perched saturation on gentle gradients and rapid loss of matric suction on steeper facets, both of which depress

factors of safety during high-intensity storms.

Sandy clay loam receives High risk because this texture combines moderate permeability with appreciable erodibility on slopes. Water moves more readily through the sandy fraction than through clay loam, which accelerates suction collapse during storm wetting, while the limited clay content provides only modest cohesion once saturated. Typical parameter compilations report reduced cohesive strength for sandy loam to sandy clay loam at saturation, consistent with the elevated class assigned in the Table.

Sandy clay receives Moderate risk because the higher clay fraction increases apparent cohesion and reduces permeability relative to sandy clay loam. The additional fine fraction delays wetting-front penetration and partially sustains matric suction, which preserves shear strength longer during a given storm, although prolonged rainfall can still generate failure once saturation develops. Studies that link soil texture to erodibility and hydraulic behavior support this intermediate assignment.

Clay loam receives Low risk because higher clay content and lower permeability generally increase shear resistance under transient wetting compared with the coarser textures. Clay-rich loams can weaken after extended saturation or where structural defects concentrate strain, yet the combination of slower infiltration, higher plasticity, and stronger apparent cohesion under typical antecedent conditions yields lower susceptibility within the local texture spectrum. The class reflects this relative behavior rather than an assumption of immunity to failure, see Table 7 and Figure 13.

Table 7: Soil Reclassification Range

Soil texture	Risk class	Rationale
Silt	5	Low cohesion and high erodibility promote shallow failures
Sandy clay loam	4	Moderate drainage with high erodibility on steep facets
Sandy clay	3	Greater clay fraction improves cohesion relative to loam
Clay loam	2	Higher cohesion and lower erodibility until prolonged saturation

Source author, 2025

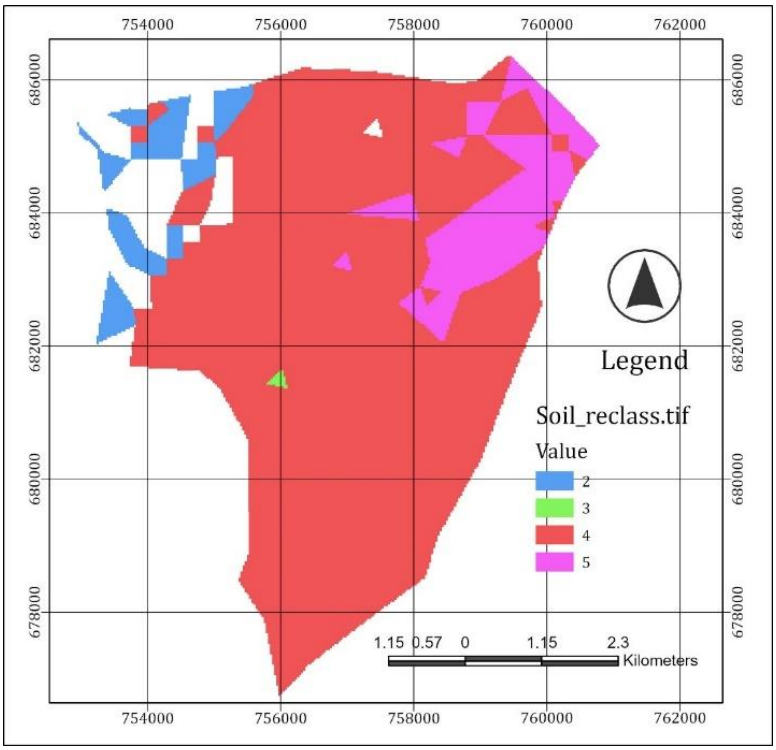

Fig 13: Reclassified Soil Data

Rainfall in the susceptibility model functions as the hydrologic forcing that raises pore water pressure in near-surface materials and lowers effective stress during storm sequences. The reclassification adopts equal intervals across the observed annual range of 2,844.26 to 2,906.37 mm to provide an ordered proxy for the likelihood that a location experiences frequent or prolonged exceedance of triggering conditions. Landslide initiation in humid terrains depends most strongly on rainfall intensity and duration, yet annual totals correlate with the frequency of high-intensity events and with cumulative wetness that controls antecedent moisture. This interpretation aligns with physically based infiltration theory and with empirical threshold studies that relate storm properties to shallow slope failure.

Very Low and Low classes in the Table correspond to the lower two quintiles of annual rainfall within the municipality. Locations in these bands experience fewer sequences where storm intensity and duration exceed local thresholds, which reduces the probability of transient saturation in colluvium and regoliths. Inventories from humid regions demonstrate that landslide incidence increases when storms cross intensity–duration thresholds, and that lower cumulative rainfall generally implies fewer threshold exceedances over a season.

The Moderate class occupies the mid-range of totals where wetting events occur frequently enough to shorten recession times between storms and to maintain higher antecedent soil moisture. Such conditions diminish matric suction before the

next intense rainfall and promote pore pressure rise during infiltration, consistent with laboratory and field evidence that shows combined control by soil properties and storm forcing on slope stability.

High and Very High classes coincide with the upper two quintiles of annual rainfall and therefore indicate the greatest probability of storm sequences that produce rapid infiltration, perched saturation, and loss of effective stress in shallow horizons. Physically based models predict accelerated timing of failure under these conditions, while threshold syntheses report a greater density of triggering events where seasonal wetness is higher. Spatial overlays in this study show that the slightly wetter southern sector aligns with several steep, concave hillslopes, which heightens susceptibility when intense storms occur, see Table 8 and Figure 14.

Table 8: Rainfall Reclassification Range

Risk class	Annual rainfall range (mm)	Rationale
1	2,844.26–2,856.68	Lowest forcing and least frequent saturation
2	>2,856.68–2,869.10	Low forcing with limited exceedance of antecedent thresholds
3	>2,869.10–2,881.53	Intermediate forcing and more frequent wetting
4	>2,881.53–2,893.95	High forcing and recurrent saturation events
5	>2,893.95–2,906.37	Very high forcing with strong probability of pore-pressure rise

Source author, 2025

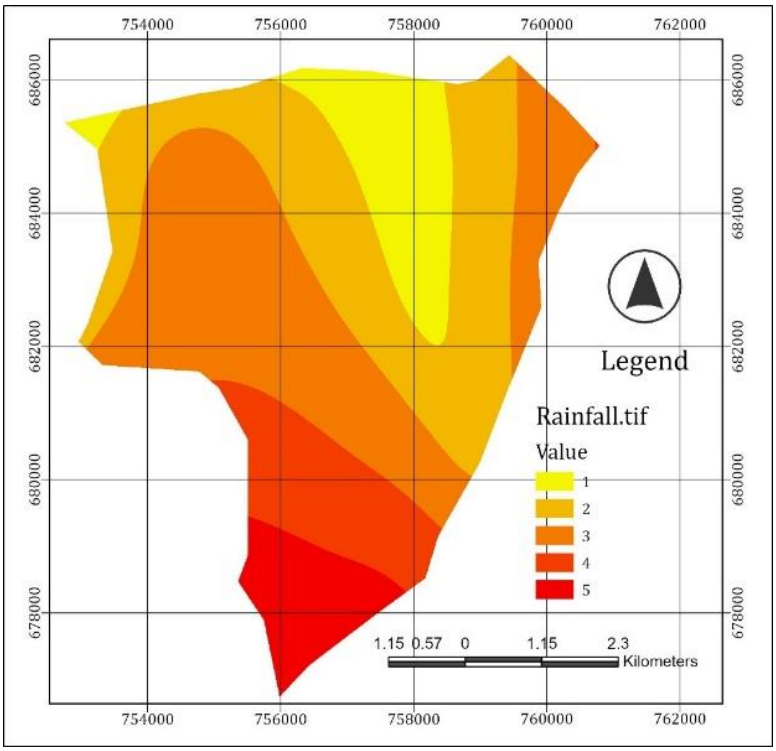

Fig 14: Reclassified Rainfall Data

3.3. Weight Derivation for Landslide Conditioning Factors

3.3.1. Pairwise Comparison Matrix

Pairwise comparison matrix was formed by inputting the judgment value between factors as the matrix elements by following the basic rules as established by Saaty. Table 9 was formulated using pairwise comparism matrix.

Table 9: Pair-wise comparison matrix of the study

	Elevation	Slope	Curvature	Aspect	Rainfall	Geology	Soil
Elevation	1	2	2	2	3	3	4
Slope	0.5	1	2	2	2	3	3
Curvature	0.5	0.5	1	2	2	3	3
Aspect	0.5	0.5	0.5	1	2	2	3
Rainfall	0.33	0.33	0.5	0.5	1	2	2
Geology	0.33	0.33	0.33	0.5	0.5	1	2
Soil	0.25	0.33	0.33	0.22	0.5	0.5	`1
Total	3.41	4.99	6.66	8.22	11	14.5	18

From Table 9, The pairwise comparison matrix synthesizes expert judgments on the relative influence of seven conditioning factors. Unity occupies the diagonal, while off-diagonal entries represent how many times the row factor is preferred over the column factor. The matrix is reciprocal by construction. Column totals (3.41, 4.99, 6.66, 8.22, 11.00, 14.50, and 18.00) indicate the overall strength of preference directed toward each factor across all comparisons.

Inspection of the matrix revealed a consistent pattern that privileges topographic controls. Elevation is judged more influential than every other factor, with preferences of 2 over Slope, Curvature, and Aspect, 3 over Rainfall and Geology, and 4 over Soil. Slope is preferred over Curvature, Aspect, Rainfall, Geology, and Soil with ratios of 2, 2, 2, 3, and 3 respectively. Curvature retains advantage over Aspect, Rainfall, Geology, and Soil, while Aspect is placed above Rainfall, Geology, and Soil but below Elevation, Slope, and Curvature. Rainfall exceeds Geology and Soil but is below all terrain metrics. Geology is preferred over Soil only. The resulting hierarchy embedded in the raw judgments is therefore Elevation > Slope > Curvature > Aspect > Rainfall > Geology > Soil.

3.3.2. Normalized Prioritization Pairwise Comparison Matrix

The normalized prioritization matrix (Table 10) was obtained by dividing each entry by its column sum so that each column sums to one. Row means of this normalized matrix yield the priority vector. The resulting weights and their percentages are Elevation 0.28 (27.71%), Slope 0.21 (20.66%), Curvature 0.17 (17.08%), Aspect 0.13 (13.29%), Rainfall 0.09 (9.13%), Geology 0.07 (7.13%), and Soil 0.05 (5.02%). The distribution confirms the dominance of terrain-derived variables in the expert assessment. Elevation and Slope account for approximately 48% of the total weight, while Curvature and Aspect contribute an additional 30%. Climatic forcing through Rainfall and material properties through Geology and Soil together account for about 21%, reflecting the view that, within this municipal setting, topographic configuration provides the primary control on landslide predisposition and that lithology and soil texture modulate this predisposition rather than drive it.

Table 10: Prioritization weight matrix

	Elevation	Slope	Curvature	Aspect	Rainfall	Geology	Soil	Mean	W%
Elevation	0.29	0.40	0.30	0.24	0.27	0.21	0.22	0.28	27.71
Slope	0.15	0.20	0.30	0.24	0.18	0.21	0.17	0.21	20.66
Curvature	0.15	0.10	0.15	0.24	0.18	0.21	0.17	0.17	17.08
Aspect	0.15	0.10	0.08	0.12	0.18	0.14	0.17	0.13	13.29
Rainfall	0.10	0.07	0.08	0.06	0.09	0.14	0.11	0.09	9.13
Geology	0.10	0.07	0.05	0.06	0.05	0.07	0.11	0.07	7.13
Soil	0.07	0.07	0.05	0.03	0.05	0.03	0.06	0.05	5.02
Total	1	1	1	1	1	1	1	1.00	100

3.3.3. Estimation of the Consistency Ratio

This stage involved calculating a consistency ratio (CR) to check reliability of the judgments values which are relative to large samples of purely random judgments. The AHP deals with consistency explicitly because in making paired comparisons, just as in thinking, people do not have the intrinsic logical ability to always be consistent.

To determine consistency ratio, the analytical hierarchy process compares it by random index (R.I.). Mathematically, Consistency Ratio (C.R.), can be defined as:

$CR = CI/RI$

In calculating the constituency value, the mathematical formula CR = CI/RI was be used.

Random index (RI) is the consistency index of a randomly generated pair-wise comparison matrix of order 1 to 10 obtained by approximating random indices.

Table 11: Random Index by Saaty

Size of matrix (n)	1	2	3	4	5	6	7	8	9	10
Random index (RI)	0	0	0.58	0.9	1.12	1.24	1.32	1.41	1.46	1.49

Source: (Saaty, 2001) [14].

Note: If the value of the obtained Consistency Ratio is less than 0.1, it means that there is a reasonable level of consistency in the pairwise comparisons, and that the computed weights are within the acceptable limit. If the reverse is the case (CR > 0.1) it means that the weights obtained are inconsistent and needs to be checked.

The value of Consistency index, CI was calculated from the preference matrix according to equation below

$$CI = \frac{\lambda max - n}{n-1}$$

λmax is the Principal Eigen Value; n is the number of factors
λmax = Σ of the products between each element of the priority vector and relative weights

$$\lambda max = (3.41 * 0.28) + (4.99 * 0.21) + (6.66 * 0.17) + (8.22 * 0.13) + (11 * 0.09) + (14.5 * 0.07) + (18 * 0.05)$$

$$= 0.95 + 1.05 + 1.13 + 1.06 + 0.99 + 1.02 + 0.9$$

$$\lambda max = 7.1$$
$$CI = (7.1 - 7)/(7 - 1) = 0.016$$
$$CR = 0.016/1.32 = 0.012$$
$$CR = 0.012 < 0.10\ (Acceptable)$$

The consistency ratio (CR) is design in such a way that if CR<0.10, the ratio indicates a reasonable level of consistency in the pairwise comparisons; if, however, CR ≥ 0.10, the values of the ratio are indicative of inconsistent judgments. From the judgment a Consistency Ratio (CR) of 0.012 was achieved which was less than the maximum allowable ratio of 0.10.

3.3.4. Sensitivity Analysis of Factor Weights

To evaluate the robustness and reliability of the AHP-derived weights used in this study, a sensitivity analysis was conducted. This analysis was essential to test whether moderate changes in factor weights would significantly alter the rankings or affect the decision outcome, thereby revealing

the degree to which the model depends on subjective expert judgments.

Seven criteria were utilized in the analysis, the original weights assigned through pairwise comparison are shown in Table 12.

Table 12: Original Factor Weights and Rankings

Factor	Original Weight	Rank
Elevation	0.28	1
Slope	0.21	2
Curvature	0.17	3
Aspect	0.13	4
Rainfall	0.09	5
Geology	0.07	6
Soil	0.05	7

Source author, 2025

From the above, it is evident that elevation emerged as the most influential factor, while soil was the least influential. To test sensitivity, the weight of each factor was varied independently by ±10% and ±20%, with proportional adjustments made to the remaining factors to ensure the total sum of weights remained equal to 1.0.

Example: Increase elevation weight by 10%

New Weight = 0.28 + (10% of 0.28) = 0.31. To keep the total = 1, the rest was adjusted proportionally as follows:

Total of other factors = 1 - 0.28 = 0.72

New total to distribute among others = 1 - 0.31 = 0.69

Adjustment Ratio = 0.69 / 0.72 ≈ 0.9583, see Table 13 for the adjusted weights.

Table 13: New Adjusted Weights (+10%)

Factor	Original	New Weight (10% ↑ LC/LU)
Elevation	0.28	0.28
Slope	0.21	0.21 × 0.9583 ≈ 0.2012
Curvature	0.17	0.17 × 0.9583 ≈ 0.1629
Aspect	0.13	0.13 × 0.9583 ≈ 0.1246
Rainfall	0.09	0.09 × 0.9583 ≈ 0.0862
Geology	0.07	0.07 × 0.9583 ≈ 0.0671
Soil	0.05	0.05 × 0.9583 ≈ 0.0479
Total	1.00	1.00

Source author, 2025

For illustration, Tables 14 and 15 show the changes in weights when the weight of elevation was increased and decreased by ±10% and ±20%, respectively.

Table 14: Weight Distribution with ±10% Change in Elevation

Scenario	Elevation	Slope	Curvature	Aspect	Rainfall	Geology	Soil
+10%	0.31	0.2012	0.1629	0.1246	0.0862	0.0671	0.0479
-10%	0.25	0.2187	0.1771	0.1354	0.0937	0.0729	0.0521

Source author, 2025

Table 15: Weight Distribution with ±20% Change in Elevation

Scenario	Elevation	Slope	Curvature	Aspect	Rainfall	Geology	Soil
+20%	0.336	0.1936	0.1567	0.1198	0.0829	0.06455	0.0461
-20%	0.224	0.2263	0.1832	0.1401	0.0969	0.0754	0.0538

Source author, 2025

Similar tests were conducted for the other six criteria. Across all scenarios, the ranking of the seven factors remained unchanged. Elevation consistently maintained its position as the most influential factor, even when its weight was reduced by 20%. Likewise, Slope and Curvature consistently held the second and third ranks, respectively. Geology, and Soil also retained their original sixth to seventh rankings across all sensitivity tests. Table 16 summarizes whether any rank changes occurred as a result of the weight perturbations.

Table 16: Summary of Ranking Stability Across Sensitivity Tests

Factor Varied	Ranking Change (±10%)	Ranking Change (±20%)	Stability Conclusion
Elevation	No	No	Very Stable
Slope	No	No	Stable
Curvature	No	No	Stable
Aspect	No	No	Stable
Rainfall	No	No	Stable
Geology	No	No	Very Stable
Soil	No	No	Very Stable

Source author, 2025

The findings from this sensitivity analysis indicate that the model is highly robust. The lack of ranking changes even under ±20% variation signifies that the results of the AHP model are not overly sensitive to subjective judgments. This consistency affirms the reliability and soundness of the factor prioritization and suggests that the urban development potential assessment derived from this model is dependable and resistant to minor input uncertainty.

3.4. Analysis of Landslide Risk Zonation

The landslide susceptibility map of Onitsha Metropolis was reclassified into four distinct zones classified by varying levels of landslide risk: Very Low Risk, Low Risk, Moderate Risk, and High Risk, see Figure 12.

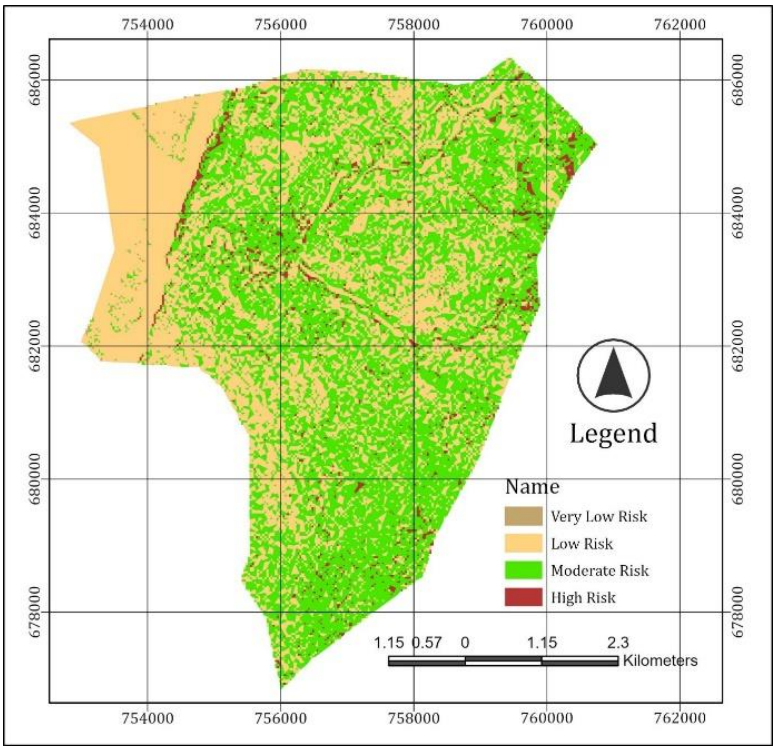

Source author, 2025

Fig 15: Landslide Risk Onitsha Metropolis

The landslide susceptibility model partitioned Onitsha Metropolis into four risk tiers that together covered 41.293 km². Moderate risk dominated the landscape and accounted for 20.985 km², representing 50.82 percent of the total area. These tracts occurred extensively across the central and eastern sectors and formed continuous belts around the drainage network. Terrain within this class typically exhibited intermediate slopes and concave elements that favoured episodic saturation. The mapped pattern indicated terrain that would experience slope instability during seasons of persistent rainfall rather than under only extreme events.

Low risk occupied 18.747 km², which corresponded to 45.40 percent. These zones formed a broad mosaic around the moderate class and were most common across gently undulating surfaces and interior interfluves. Terrain attributes suggested adequate drainage, lower relief, and limited hydrologic convergence. Settlement expansion and linear infrastructure located within these areas would face comparatively lower exposure to landslide processes, although localized hazards could still arise near channel margins and cut slopes.

High risk covered 1.414 km², which amounted to 3.42 percent. These cells appeared as narrow, elongated clusters along steep valley flanks, headwater hollows, and break-of-slope rims. Spatial coincidence with strong curvature and higher gradients implied short warning times during intense storms and a propensity for shallow translational failures. Sites within this tier warranted field verification, targeted slope management, and closer design controls for earthworks.

Very low risk was limited to 0.147 km², or 0.36 percent. These fragments corresponded to nearly planar ground in valley bottoms and broad terraces. Slope-parallel gravitational forcing was minimal, and instability would more likely be associated with bank undercutting or anthropogenic excavation than with hillslope failure.

The relative area shares showed a municipality where susceptibility was widespread but generally moderate, with a small fraction of high-risk corridors that concentrated along the hydrographic framework. The partitioning aligned with the mapped conditioning factors and supported a management strategy that prioritized monitoring and mitigation along the limited high-risk tracts while guiding routine development toward the extensive low- and moderate-risk belts under appropriate site-scale checks.

The spatial extents of each zone were calculated in square kilometers and are presented alongside their corresponding percentage coverage in Table 17.

Table 17: Area Coverage of Landslide Risk Zones

Landslide Risk Zone	Area (km²)	Percentage (%)
Very Low Risk	0.147	0.36
Low Risk	18.747	45.40
Moderate Risk	20.985	50.82
High Risk	1.414	3.42

The spatial distribution of landslide susceptibility across Onitsha Metropolis revealed distinct patterns when specific localities were overlaid on the risk map. This locational analysis provided further insight into the geomorphic vulnerability of particular neighbourhoods and supported targeted risk management interventions.

Areas such as GRA, Okpoko, the Army Barracks, and Nkwelle were mapped within the high-risk zone. These neighbourhoods occupy terrain characterized by steep topographic gradients, high relative relief, and pronounced planform or profile curvature. In addition, several of these

sites coincide with known cut-and-fill zones, road embankments, or artificial slopes resulting from rapid urban development. For instance, Okpoko and the Army Barracks lie along the north western corridor where elevation differentials are abrupt, and vegetation removal has been intensive. Nkwelle, similarly, occupies elevated terrain with frequent hydrological concentration, making it highly susceptible to slope failure during periods of prolonged precipitation. Within GRA, modifications of the natural landscape and drainage patterns often due to residential construction and road development have exacerbated the terrain's sensitivity to saturation and overland flow-induced failures. The concentration of these high-risk localities within the high-risk class indicates zones where intervention strategies should prioritize early warning systems, slope stabilization works, drainage enhancement, and enforced land-use regulation.

Conversely, localities such as Trans Nkisi, Umuaroli, Omogba, Fegge, and Odoakpu were predominantly situated within the moderate-risk zone. These areas exhibited a more balanced interaction between natural topographic features and anthropogenic alterations. Moderate slope inclinations, relatively stable geological substrates, and partial vegetation cover contributed to intermediate susceptibility. However, urban expansion, impervious surface proliferation, and unmanaged runoff have introduced conditions favorable to localized failures, particularly near steepened road cuttings and drainage-constrained neighbourhoods. In Trans Nkisi and Fegge, for example, built-up surfaces overlay gently sloping terrain, but heavy rainfall events may still pose a threat where water is not properly channelled. Similarly, Umuaroli and Odoakpu contain flat to undulating zones with low geomorphic energy, yet the combination of land-use pressure and hydrological variability elevates their risk profile to a moderate level.

These spatial associations underscored the heterogeneity of landslide susceptibility across the LGA. High and very high-risk zones were often associated with localized terrain amplification, especially along escarpments, foot slopes, or concave zones with water convergence. Moderate-risk areas extended across transitional surfaces and low hills where landform and human influence combined to moderate the landslide hazard. This mapping outcome highlighted the need for a location-specific risk reduction framework in which very high-risk neighbourhoods receive immediate mitigation attention, while moderate-risk zones benefit from integrated planning that includes drainage improvement, land-use regulation, and slope management measures.

4. Conclusion

The landslide susceptibility analysis conducted for Onitsha Metropolis provided an evidence-based evaluation of spatial risk distribution using a combination of geospatial modeling, statistical weighting, and expert-based multi-criteria evaluation. The results demonstrated a clear variation in susceptibility levels across the region, with the majority of the area falling within moderate (50.82%) and low (45.40%) risk classes. However, the presence of high (3.42%) and very low (0.36%) risk zones highlights the geomorphic complexity of the area and the spatial concentration of instability in specific localities.

The spatial overlay analysis further revealed that neighbourhoods such as GRA, Okpoko, the Army Barracks, and Nkwelle fall within very high-risk zones, where steep slopes, high curvature, and intense anthropogenic modifications converge to produce a landscape that is highly susceptible to failure during hydrometeorological events. These areas represent priority targets for mitigation, slope stabilization, and policy enforcement. Conversely, localities such as Trans Nkisi, Umuaroli, Omogba, Fegge, and Odoakpu, although situated in moderate-risk zones, require strategic management to limit future transitions into higher risk classes due to ongoing urban expansion and drainage challenges.

The study established a comprehensive and spatially explicit framework for understanding landslide susceptibility in Onitsha Metropolis. The outcomes offer critical guidance for land-use planners, environmental managers, and disaster risk reduction agencies by delineating zones of varying susceptibility and identifying neighborhoods requiring immediate attention. Future work should integrate temporal landslide occurrence data and field validation to further refine susceptibility predictions and to develop early warning systems tailored to the geomorphic and socio-infrastructural realities of the area

References

1. Amah VE, Egboka BCE, Okeke HC, Nwankwoala HO. GIS and statistical based assessment of landslide susceptibility in southeastern Nigeria. Environ Earth Sci. 2020;79(14):1–16.
2. Ayadiuno RU, Ndulue EL, Mozie AT, Ndichie CC. Machine learning approaches for landslide susceptibility mapping in southeastern Nigeria. Arab J Geosci. 2021;14(18):1–20.
3. Hall JW, Huang H, Timokhin D, Hammel N. Global natural hazard risk assessment and urban resilience analysis using geospatial technologies. Int J Disaster Risk Reduct. 2020;50:101714.
4. Ifeka AC, Akinbobola A. Rainfall variability and climatic characteristics of southeastern Nigeria. J Geogr Reg Plan. 2015;8(5):98–107.
5. Luo X, Chen G, Zhang L, Wang H. Urbanization effects on slope instability and hydrological response in rapidly developing cities. Sustainability. 2022;14(9):5321.
6. Metternicht G, Hurni L, Gogu R. Remote sensing of landslides: An analysis of the potential contribution to geospatial systems for hazard assessment in mountainous environments. Remote Sens Environ. 2005;98(2–3):284–303.
7. Nebeokike SC, Igwe O, Egbueri JC, Ifediegwu SI. Landslide susceptibility modelling using Naïve Bayes algorithm and GIS techniques in southeastern Nigeria. Model Earth Syst Environ. 2020;6(4):2345–2360.
8. Nnadi EO. Climatic variability and rainfall characteristics in Anambra State, Nigeria. J Environ Earth Sci. 2019;9(4):45–56.
9. Nnanwuba CC, Nwosu JI, Okeke FI, Ezeh CU. Comparative analysis of machine learning techniques for landslide susceptibility mapping in southeastern Nigeria. Geocarto Int. 2022;37(12):3501–3520.
10. Obeta MC. Rainfall intensity and environmental implications in southeastern Nigeria. J Hydrol Reg Stud. 2022;41:101066.
11. Okeke FC, Eze JN, Nwankwo CO. Urban climate characteristics and rainfall variability in Onitsha Metropolis, Nigeria. Afr J Environ Sci Technol. 2019;13(6):221–232.

12. Oloruntade AJ. Seasonal rainfall variability and runoff generation in southeastern Nigeria. Hydrol Sci J. 2018;63(11):1657–1670.
13. Ozioko RE, Igwe O. GIS-based heuristic and bivariate statistical modelling of landslide susceptibility in Iva Valley, southeastern Nigeria. Environ Monit Assess. 2020;192(9):1–19.
14. Saaty TL. Decision making with dependence and feedback: The analytic network process. 2nd ed. Pittsburgh: RWS Publications; 2001.
15. Ulakpa ROE, Okwu VI, Chukwu KE, Eyankware MO. Application of GIS and remote sensing in landslide susceptibility mapping and hazard assessment. Int J Sci Technol Res. 2020;9(3):5404–5412.

How to Cite This Article

Nkanu BI, Emengini EJ, Idhoko KE. Mapping landslide susceptibility areas in Onitsha Metropolis of Anambra State Nigeria using GIS. Int J Multidiscip Res Growth Eval. 2026 May–Jun;7(3):452–471.

Creative Commons (CC) License